analytical chemistry

pubs.acs.org/ac Article

Boreas: A Sample Preparation-Coupled Laser Spectrometer System for Simultaneous High-Precision In Situ Analysis of $\delta^{13}C$ and $\delta^{2}H$ from Ambient Air Methane

Chris Rennick, Tim Arnold,* Emmal Safi, Alice Drinkwater, Caroline Dylag, Eric Mussell Webber, Ruth Hill-Pearce, David R. Worton, Francesco Bausi, and Dave Lowry

Cite This: *Anal. Chem.* 2021, 93, 10141−10151 Read Online

ACCESS | Metrics & More | Article Recommendations | Supporting Information

ABSTRACT: We present a new instrument, "Boreas", a cryogen-free methane (CH_4) preconcentration system coupled to a dual-laser spectrometer for making simultaneous measurements of $\delta^{13}C(CH_4)$ and $\delta^{2}H(CH_4)$ in ambient air. Excluding isotope ratio scale uncertainty, we estimate a typical standard measurement uncertainty for an ambient air sample of 0.07‰ for $\delta^{13}C(CH_4)$ and 0.9‰ for $\delta^{2}H(CH_4)$, which are the lowest reported for a laser spectroscopy-based system and comparable to isotope ratio mass spectrometry. We trap CH_4 (~1.9 μmol mol^{-1}) from ~5 L of air onto the front end of a packed column, subsequently separating CH_4 from interferences using a controlled temperature ramp with nitrogen (N_2) as the carrier gas, before eluting CH_4 at ~550 μmol mol^{-1}. This processed sample is then delivered to an infrared laser spectrometer for measuring the amount fractions of $^{12}CH_4$, $^{13}CH_4$, and $^{12}CH_3D$ isotopologues. We calibrate the instrument using a set of gravimetrically prepared amount fraction primary reference materials directly into the laser spectrometer that span a range of 500−626 μmol mol^{-1} (CH_4 in N_2) made from a single pure CH_4 source that has been isotopically characterized for $\delta^{13}C(CH_4)$ by IRMS. Under the principle of identical treatment, a compressed ambient air sample is used as a working standard and measured between air samples, from which a final calibrated isotope ratio is calculated. Finally, we make automated measurements of both $\delta^{13}C(CH_4)$ and $\delta^{2}H(CH_4)$ in over 200 ambient air samples and demonstrate the application of Boreas for deployment to atmospheric monitoring sites.

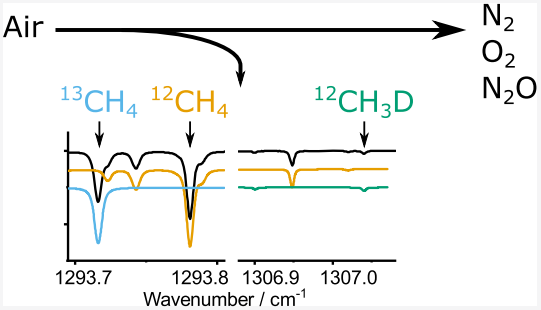

1. INTRODUCTION

Methane (CH_4) concentrations in the atmosphere have more than doubled over the last 150 years, and the contribution to increased radiative forcing since the industrial revolution is around a quarter of that relative to carbon dioxide (CO_2).[1] Mitigation of CH_4 emissions therefore plays a vital role in tackling the climate crisis. Unlike CO_2 that has shown a very consistent rise in the atmosphere over the last century, owing to anthropogenic fossil fuel emissions, CH_4 has gone through periods of small changes in the growth rate for reasons that are poorly understood.[2] Methane is emitted from a variety of sources and processes and removed largely by chemical destruction in the troposphere (global atmospheric lifetime of ~decade). Although anthropogenic emissions have been a clear main driver of the rising global atmospheric concentrations over the last century, the sectoral (e.g., agricultural vs energy), temporal, and spatial disaggregation of emissions remains poorly quantified and difficult to verify through atmospheric measurements of amount fractions alone.[3] While the main thrust of the widespread mitigation measures needed is very clear (elimination of fugitive leaks during fossil fuel extraction and transport and development of low-emission agricultural methods), the measurement tools to aid timely, efficient, and equitable policy decision making are lacking.[3]

Different formation, transport, and removal processes can impart distinctive isotopic fractionations on molecules.[4] These naturally occurring isotopic labels provide an extra layer of information for studying biogeochemical cycling and anthropogenic emissions.[3,5] Isotopic composition, typically measured by isotope ratio mass spectrometry (IRMS), has provided key insights into our understanding of the historical and contemporary global atmospheric budgets.[5] Isotopic records are largely constructed by continuous or one-off sampling campaigns followed by analysis in the laboratory by IRMS.[6] The high-quality measurements needed for such studies are difficult to make, time-consuming, expensive, and only performed by less than 20 laboratories across the world.[7] In

Received: March 13, 2021
Accepted: June 23, 2021
Published: July 14, 2021

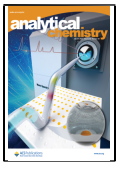

https://doi.org/10.1021/acs.analchem.1c01103
Anal. Chem. 2021, 93, 10141−10151

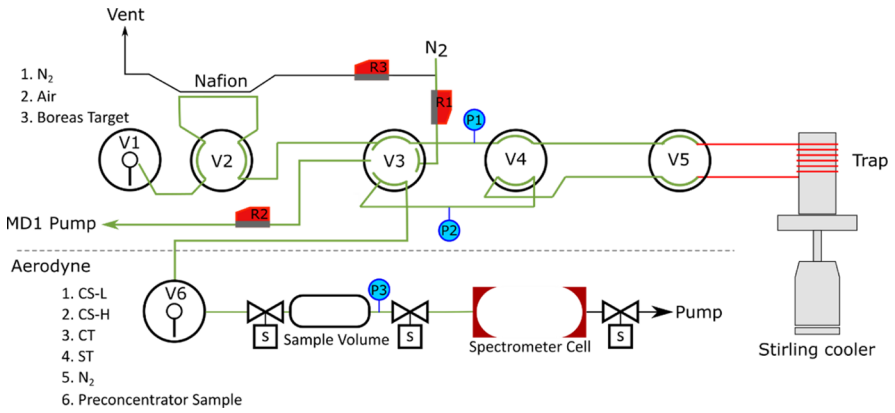

Figure 1. Flow scheme for the sampling of CH_4 from ambient air and delivery to the laser spectrometer. Valves 1−6 (V1−V6), mass flow controllers (R1−R3), and pressure transducers (P1−P3) are labeled. The solenoid valves are denoted by a squared "S". The sampling volume and spectrometer cell are notated in the figure. Multi-selector V1 has three ports connected; (1) N2; (2) air; and (3) the Boreas target (BT). Multi-selector V6 has six ports connected that lead to the spectrometer; (1) low-calibration standard AF PRM (CS-L); (2) high-calibration standard AF PRM (CS-H); (3) calibration target AF PRM (CT); (4) spectrometer target AF PRM (ST); (5) pure N_2; and (6) sample from the trap. The dotted line indicates the separation of control between the preconcentrator and spectrometer software.

populated regions, such as Europe, different types of emission sources are in proximity, making it difficult to usefully verify emissions (i.e., quantitative separation of different sources) using atmospheric measurements. However, in bringing together the source-specific information gained from isotopic observables and the benefits of coupling high-frequency measurements with high-resolution atmospheric chemistry transport model (ACTM) outputs, we will be able to make a significant improvement in our quantitative understanding of sector-specific fluxes.[8,9] To this end, impressive attempts have been made to take IRMS systems to atmospheric observatories for high-precision, in situ, frequent analysis of both $\delta^{13}C(CH_4)$ and $\delta^2H(CH_4)$.[9−11] These studies generated thousands of measurements over many months, providing data that could be assimilated into ACTMs for interpretation.

Instruments (such as Fourier-transform infrared or laser absorption spectrometers) can make high-frequency measurements with potentially lower maintenance requirements, therefore allowing atmospheric monitoring at greater spatial coverage. However, commercial spectrometers are unable to make sufficiently high-precision $\delta^{13}C(CH_4)$ and $\delta^2H(CH_4)$ measurements due to the low abundance of CH_4 in ambient air, which results in a poor signal-to-noise ratio (currently dry air amount fractions in the well-mixed atmosphere are <2 μmol mol^{-1}). One method to improve the signal-to-noise ratio is to concentrate the analyte of interest out of ambient air for analysis with a commercially available spectrometer. Eyer et al.[12] made progress in developing this approach for simultaneous measurements of $\delta^{13}C(CH_4)$ and $\delta^2H(CH_4)$ by laser spectroscopy and later showed the potential for these more efficient measurement systems to be deployed.[9] The measurement repeatability (0.19‰ for $\delta^{13}C$ and 1.9‰ for δ^2H), however, was significantly larger than that of laboratory-based IRMS methods (<0.05‰ for $\delta^{13}C$ and 1‰ for δ^2H). This study also highlighted significant problems for analysis that included the potential for breakthrough on traps (due to the large sample volume needed) and the issue of variable oxygen (O_2) content of the trapped sample that continues on to create a matrix effect in analysis by laser spectroscopy.

In this work, we describe the design of a new robust preconcentration system coupled to a dual-laser spectrometer and demonstrate several weeks of continuous operation alternating between ambient air samples and whole air reference standards. Alongside this, we describe a rigorous and efficient calibration procedure for isotopologue ratio measurements from ambient air samples—the first demonstration of an isotopologue amount fraction-based calibration scheme for CH_4 using synthetic gravimetrically prepared standards.

2. METHODS

2.1. Overview. The limitations to use infrared laser absorption spectroscopy for isotope ratio measurement of atmospheric CH_4 arise from the weak signals due to low ambient amount fractions and interference from other gases. Boreas tackles this problem by physically separating interferences while increasing the amount fraction in the sample that is then introduced into the spectrometer.

Boreas is constructed from three distinct connected parts: (1) a purpose-built unit for sampling, CH_4 preconcentration, and interference removal; (2) a sampling interface to prepare the gas sample for the spectrometer; and (3) a mid-infrared dual-laser spectrometer. Calibration of the spectrometer is performed separately with amount fraction primary reference materials (AF PRMs) of CH_4 in nitrogen (N_2). Whole air target gas working standards are treated the same as an air sample and used to perform a final correction to the spectrometer-only calibration. The system is fully automated and alarmed, allowing continuous remote operation for weeks with high-purity N_2 carrier gas and standard gases as the only consumables.

2.2. Instrument Description. *2.2.1. Laser Spectrometer.* The spectrometer is a commercial high-resolution dual-laser direct absorption instrument (Aerodyne Research, Inc, TILDAS-FD-L2). The wavelength of a pair of quantum cascade lasers is swept sequentially over two frequency ranges: 1293.702−1293.816 cm^{-1} for $^{12}CH_4$ and $^{13}CH_4$ and 1306.883−1307.077 cm^{-1} for $^{12}CH_4$ and $^{12}CH_3D$. The resulting spectrum is fitted for the amount fraction of the isotopologues using parameters from the Hitran2016 database[13] and a polynomial baseline. Details are given in the Supporting Information S1.

2.2.2. Sampling and Preconcentration. The sampling and preconcentration unit was custom-built at the National

https://doi.org/10.1021/acs.analchem.1c01103
Anal. Chem. 2021, 93, 10141−10151

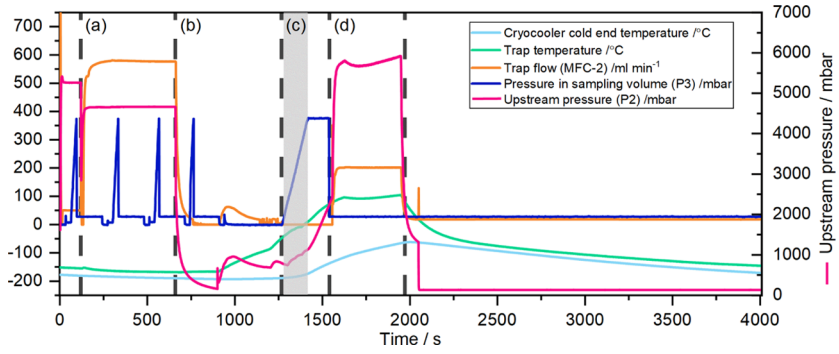

Figure 2. Stripchart of various instrument parameters during a run. Left axis: cryocooler cold-end temperature; trap temperature (thermocouple attached midway on the outside of the trap tubing); trap flow (recorded using the mass flow controller downstream of the trap); and sampling volume pressure (Figure 1, P3): The sampling volume pressure's four peaks between 0 and 750 s are loading of the standards, independent of the preconcentrator operation. Right axis: upstream pressure (Figure 1, P1). Vertical dashed lines mark the boundaries of each phase (a) trapping, (b) CH_4 separation, (c) CH_4 elution, and (d) reconditioning.

Physical Laboratory (NPL), UK. A schematic of the sample flow scheme is shown in Figure 1. The core piece of hardware is a cryocooler (CryoTel GT Sunpower Inc., USA) that is able to reach temperatures of <40 K with minimal heat load and at 100 K has a lift of >20 W. The cold end of this cryocooler is housed in a vacuum for thermal isolation (below 10^{-6} mbar pumped using an Edwards nEXT85D turbomolecular pumping station), interfaced with the sample gas via a trap tube (stainless steel, 1.5 m long, 1/8″ outside diameter, 2.0 mm inside diameter) containing the HayeSep-D (1 m packed length of 100/120 mesh) with a 250 mm void at each end (Thames Restek UK Ltd). Thus, the volume of 100/120 mesh HayeSepD is calculated as 3142 mm^3, which is comparable to that of other systems such as the Medusa GC−MS and TREX, which have trapping volumes of 1544 and 6363 mm^3, respectively.[12,14,15] The trap tube is wrapped around a cylindrical standoff permanently attached to the cold end of the cryocooler in a manner similar to previous designs[14−16] and heated resistively via a custom-built variable-voltage power supply unit. The temperature of the trap is monitored using a pair of thermocouples (TCs) affixed to both the trap tubing and the inside of the standoff. Valves 1−6 are VICI Valco GC valves with electronic actuators: valves 1 and 6 are 6-port multi-selector models (VIEUTA-2LCSD6UWEPH) for connection of Boreas and Aerodyne sample and standard gases, respectively. Valves 2, 4, and 5 are 4-port 2-position models (VIEUDA-2C4UWEPH); valve 3 is a 6-port valve with a special rotor engraving and a 12-position motor that can direct the gas during the sampling sequence between the sample, trap, N_2 flush, and spectrometer (VIEUDA-2C6UWEPH-SI2). Valve 4 controls the flow direction through the trap, and valve 5 acts to isolate the trap from the rest of the gas manifold. Flow rates are controlled using mass flow controllers (MFCs) 1−3 (Red-Y, GSC-B3SA-BB22). The pressure drop across the trap is monitored using two absolute pressure transducers (Sensors One, DTC 531).

The timing of events in a single sampling cycle is shown in Figure 2 and consists of four phases, trapping, CH_4 separation, CH_4 elution, and trap reconditioning, before the trap is allowed to cool for the next cycle.

2.2.2.1. Trapping (0−660 s). The ambient air sample is brought to the head of the trap using a sampling pump (N143 Series, KNF Neuberger UK Ltd, UK) with an outlet pressure of 4.5 bar, controlled using a backpressure regulator, creating a flow rate downstream of the trap measured using MFC-2 of ∼580 mL min^{-1} (STP); the pressure of the whole air standard is set using a cylinder-mounted regulator. The sample gas is dried using a Nafion dryer with a N_2 (Air Products, BIP purity) counterpurge at a flow rate of 200 mL min^{-1} during sampling and 20 mL min^{-1} when not sampling, set using MFC-3. Valve 4 is set to forward flow the sample through the trap, and V3 is set to direct the effluent to vent through R2 (this also isolates V6 and the spectrometer from the preconcentrator). V5 is initially set so the flow bypasses the trap, allowing the rest of the system to purge with the sample. After 2 min of flow to purge the valve system, the bypass valve V5 opens to the trap, which can be seen as the step change in flow and pressure at the start of phase (a) in Figure 2. The sample flows through the trap starting at ∼113 K without any active heating but while the trap is still cooling from the previous run. Trapping continues for 540 s during which the trap cools by a further 10 K reaching a final temperature of 103 K at the end of trapping. The trapping temperature does not need to be controlled by any active heating (trapping temperature repeatability between cycles is <1 K). Trace gases from around ∼5 L of air (STP) are trapped on the adsorbent by the end of sampling; the integrated volume is recorded for each run from the flow measured using MFC-2.

During phases (a,b), the spectrometer is successively filled with four of the high-amount fraction mixtures, and the spectra were recorded for 100 s. These gases flow through the sampling volume in order to match the pressure of the trap sample, and this can be seen as the spikes of pressure in the sampling volume plotted in blue in Figure 2.

2.2.2.2. Methane Separation (660−900 s). After 540 s, sampling is discontinued by moving the sample selector V1 to a blanked inlet and letting the trap decompress by pumping out through MFC-2 for 240 s. This decompression reduces the dead volume of gas in the system and the trap and limits the backward expansion of the sample at the onset of heating. At 900 s, the trap is heated from 103 K to 373 K over 720 s. During this period, the trap is forward flushed (still to vent through MFC-2) at a flow rate of 6 mL min^{-1} and then 10 mL min^{-1} with N_2 (controlled with the MFC-1).

2.2.2.3. Methane Elution (1260−1410 s). At ∼360 s into the temperature ramp, V3 steps position to divert the trap effluent to the 50 mL sampling volume (Swagelok stainless-steel miniature sample cylinder). Once the pressure reaches 375 mbar, the sampling volume is shut off. This filling can be seen as the rising pressure in the sampling volume during

https://doi.org/10.1021/acs.analchem.1c01103
Anal. Chem. 2021, 93, 10141−10151

phase (c) plotted as a blue line in Figure 2. The exact timing of the valve steps is optimized to capture all eluted CH_4 into the sampling volume (see Section 2.3.2).

2.2.2.4. Reconditioning (1620−1950 s). At the end of the CH_4 elution step, V3 steps to the third position, and the trap effluent returns to vent. At this point, the trap has reached over 273 K, and the ramp continues to 373 K and is maintained for 300 s, while the trap is reconditioned by the purging of less volatile species (most significantly H_2O). The heating is then cut off, and the trap is allowed to cool passively via the dissipation of heat through the cryocooler.

2.2.3. Sampling−Spectrometer Interface and Instrument Control. The sampling system is fully automated and controlled using GCWerks (GCSoft Inc) on a Linux-based computer. Once the CH_4 has been transferred into the sampling volume, control passes to the laser spectrometer software, TDLWintel (Aerodyne Research Inc), and the gas mixture in the sampling volume is equilibrated with the 500 mL cell (previously evacuated) within the laser spectrometer for measurement of the three isotopologue abundances. On completion of the measurement (see Section 3.1 below), the sampling volume and cell are evacuated in preparation for calibration of the instrument using synthetic standard gases (see Section 2.3 below).

Each sample from an AF PRM or from the trap is loaded into the spectrometer and is automatically analyzed using the spectrometer software. The trap eluent contains varying amounts and possibly different isotopic compositions of CH_4 (see period c in Figure 2), along with other gases that are being removed from the trap at the same time (see Section 3.2), so the mixture is allowed to homogenize in the sample volume for 2 min. The preconcentrated sample or AF PRM sample is first loaded into the sample volume at 375 mbar. The solenoid valve downstream of the sampling volume then opens, allowing the mixture to expand into the spectrometer cell to a final pressure of 28.5 mbar.

2.3. Measurement Protocols and Calibration Methodology. *2.3.1. Laser Spectrometer Measurement Acquisition.* Once in the laser spectrometer cell, the mixture is given 30 s to equilibrate thermally, during which the instrument response changes as the gas warms to the cell temperature. After equilibration, the spectrum is recorded at 1 s intervals, and each spectrum is fitted for an amount fraction. This gives 100 s of reported amount fraction data, which are then averaged to give the measurement for each sample. This optimum averaging time was determined from the minimum in the Allan variance, which indicates the period that the signal is affected by random noise rather than systematic drift. Details of the spectrometer stability and optimum averaging time are given in Supporting Information S2.

2.3.2. Optimization of CH_4 Elution from the Trap. Quantitative capture of CH_4 from the trap is essential in order to prevent isotopic fractionation while preventing co-elution of possible spectroscopic interfering analytes that can vary in amount in ambient air (e.g., nitrous oxide, N_2O). To this end, we also use the HaysepD trap as a chromatographic column by fore-flushing CH_4. This allows volatile gases such as O_2 to be largely removed before elution of CH_4, while variable and less-volatile gases such as N_2O remain on the trap until later in the temperature ramp. We optimized the system by sampling the trap effluent at different transfer time delays with respect to the start of the temperature ramp 10 s apart in a set of otherwise identical runs. This is necessary in our system (closed spectrometer vs flow through), whereby the elution profiles of analytes cannot be measured directly in real time. The sample volume fills to the same 375 mbar pressure in each of these runs with the flushing N_2. The CH_4 amount fraction as a function of time delay effectively shows the time profile for CH_4 elution, but the shape of this peak is broadened by the approximately 100 s that the valve is opened. We perform a simple deconvolution of this "instrument function" to recover an estimate of the elution profile by taking the difference between the CH_4 amount fractions from two consecutive runs and dividing this by the difference in transfer time delay between the runs (10 s). Figure 3 plots this estimate for the

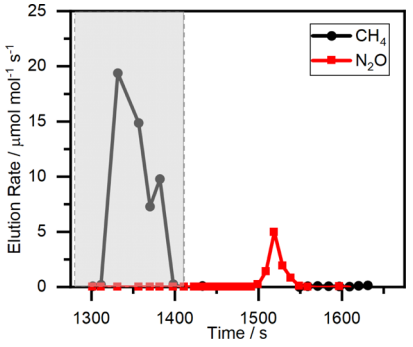

Figure 3. Elution profile of CH_4 and N_2O from the trap, reconstructed by a deconvolution procedure described in the text. Each point is a separate instrument cycle, and the spectrometer measures CH_4 and N_2O simultaneously for each sample. The time axis is relative to the start of the cycle (Figure 2), and the shaded region indicates the valve timing selected as the optimum during which the sample volume is filled.

CH_4 and N_2O spectrometer signals for a set of different transfer time delays. This demonstrates that the chosen transfer delay time and duration (represented by the gray shading) completely enclose the CH_4 elution profile and that there is significant separation (~90 s) between the end of CH_4 elution and the start of that of N_2O, allowing the sampling volume to be closed off before N_2O elution.

We analyzed the composition of the Boreas trap effluent (collected under optimized conditions) for other major gases that were concentrated and eluted together with CH_4 but are not visible to the laser spectrometer. The preconcentrator was allowed to sample from the Boreas target whole air standard (Table 1); however, instead of transferring to the sampling volume for equilibration and injection into the spectrometer, the trap effluent was captured into a different 50 mL gas cylinder fitted with a valve for removal and offline analysis. The effluent has a nominal composition of approximately 550 μmol mol^{-1} CH_4 in the pure N_2 carrier gas plus trace amounts of other air components more volatile than CH_4 such as O_2, argon (Ar), and krypton (Kr). This captured effluent sample was transferred to an evacuated 10 L (water volume) gas cylinder and diluted in helium (He) (Air Products, BIP) to pressurize the mixture for analysis by gas chromatography. The dilution factor from He addition is estimated as 0.02% from the accurate mass of each addition determined by gravimetry and assuming that the eluant is pure N_2 for the purpose of estimating molecular mass. The permanent gas components were separated using two capillary columns (2 × molsieve 5A, 30 m × 0.53 mm × 0.50 μm), and detection was on a pulsed-discharge He ionization detector (PDHID). By comparison

https://doi.org/10.1021/acs.analchem.1c01103
Anal. Chem. 2021, 93, 10141−10151

Table 1. Prepared Gas Standards (AF PRMs and Whole Air) Used to Calibrate and Characterize the Performance of Boreas[a]

sample name (NPL ID)	CH_4 origin (NPL ID)	description	CH_4 (μmol mol^{-1})	NPL Boreas		externally measured or assigned values		
				$\delta^{13}C$ (1SD, n) (‰)	$\delta^{2}H$ (1SD, n) (‰)	$\delta^{13}C$ (1SD, n) (‰)	$\delta^{2}H$ (1SD) (‰)	$\delta^{13}C$ Boreas offset (‰)
CS-L (NPL-2635)	CK gases (A462)	low-calibration standard AF PRM	500.1	n/a[b]	n/a	−51.50	−192.70	n/a
CT (NPL-A662)	CK gases (A462)	calibration target AF PRM	549.9	−51.54 (0.06, 116)	−192.66 (0.29, 116)	−51.50	−192.70	n/a
CS-H (NPL-A659)	CK gases (A462)	high-calibration standard AF PRM	625.5	n/a	n/a	−51.50	−192.70	n/a
ST (NPL-2833)	Air Products (25977)	spectrometer target AF PRM	599.9	−41.45 (0.06, 116)	−190.46 (0.29, 116)	−41.27	n/m	0.18
ST-d (NPL-3059)	Air Products (25977)	near-ambient spectrometer target AF PRM for IRMS analysis	2.490	n/m[c]	n/m	−41.27 (0.06, 12)	n/m	n/a
CS-d (NPL-2550)	CK gases (A462)	near-ambient calibration AF PRM for IRMS analysis	2.006	n/m	n/m	−51.50 (0.04, 12)	−192.70	zero (anchor point)
BT (H-356)	ambient air (Mace Head-filled June 2018)	whole air Boreas target	1.908	−47.15 (0.08, 58)	−92.63 (1.32, 58)	n/m	−92.63	n/m
H-354	ambient air (Mace Head-filled June 2018)	whole air IRMS/Boreas intercomparison sample	1.916	−47.15 (0.06, 26)	−94.79 (0.84, 25)	−47.41 (0.04, 12)	n/m	0.26

[a]Where an uncertainty is provided, it indicates a $\delta^{13}C$ direct measurement of that sample either by IRMS (measured by the RHUL, as described in Supporting Information S4) or using Boreas (using the isotope ratio anchor points of NPL-2550, as described in Section 2.3). [b]n/a = not applicable as CS-H and CS-L are not measured with Boreas but used as the "known" calibration standards with assigned isotope ratios. [c]n/m = not measured.

with NPL in-house standards, the amount fraction of O_2 in the sample was calculated as (10 ± 1) mmol mol^{-1}. The concentrations of other permanent gases (Kr and Ar) in the sample were <0.5 mmol mol^{-1}.

2.3.3. Isotope Ratio Calibration. The accuracy of molecular spectroscopy measurements made using a laser spectrometer depends on either the excellent characterization of the matrix effect (line broadening, etc.) or preparation of standards that contain the same matrix and interfering components as the sample of interest. Differences in the composition of both the calibration gases and sample lead to differences in the instrument response that will create a bias in the calibrated amount fraction. The process of concentrating CH_4 necessarily leads to alteration of the ambient air matrix, that is, the proportion of O_2 to N_2 and noble gases. We therefore aimed to concentrate CH_4 from air on the trap and then remove the CH_4 from the trap with pure N_2 carrier gas.

This approach has significant potential for developing a long-term, simplified, and traceable calibration strategy: if the CH_4 from air can be transferred to a pure-N_2 matrix (i.e., the preconcentrator both boosts the sensitivity of the spectrometer and removes pressure-broadening interferences), then, synthetic AF PRMs alone can be used to calibrate Boreas. This approach lends itself particularly well to calibration of a laser spectrometer. In theory, the spectrometer can be calibrated using only a set of standards with different well-known amount fractions but with identical isotopic composition. As long as the linearity of the instrument is well characterized, memory effects in the instrument are negligible, and the calibration gases hold the same matrix as the sample, then, an accurate isotope ratio measurement can be made.[17,18]

2.3.4. Calibration Standards and Targets. Two high-AF PRMs prepared from CH_4 in N_2 were used as calibration standards for the spectrometer by directly filling the cell: calibration standard low and calibration standard high (CS-L and CS-H, respectively). Two more high-AF PRMs are used to validate the spectrometer calibration: one named as the calibration target (CT) containing CH_4 from the same source as CS-L and CS-H and the other named as the spectrometer target (ST) containing CH_4 from a different parent batch. Two compressed whole air samples (BT and H-354) were used to calibrate and characterize Boreas's performance by sampling through the preconcentrator. Two other AF PRMs for analysis by IRMS were prepared, with a near-ambient CH_4 amount fraction, by diluting the CT and ST by further addition of N_2.

Table 1 provides a full list of samples and mixtures together with the sample name and description, and Figure 4 shows the relationship between the parent CH_4 source and the mixtures prepared for measurement using Boreas and IRMS. The AF PRM calibration standards (CS-L and CS-H) and calibration target (CT) were prepared gravimetrically by diluting a 2.23% CH_4 (N6.0, CK gases) parent standard to 500, 626, and 550 μmol mol^{-1}, using high-purity N_2 (N6.8-grade BIP+, Air Products). The CH_4 for the ST came from another source (25977 technical-grade 2.5, Air Products) diluted to 600 μmol mol^{-1} using the same high-purity N_2. These synthetic AF PRMs allowed us to calibrate and assess the performance of the spectrometer alone, and BT and H-354 are used to characterize the performance of the full Boreas system. These cylinders (50 l water volume, aluminum Luxfer gas cylinders, Matar, Italy) were filled at the Mace Head Observatory using an oil-free compressor (RIX Industries) following the National Oceanographic and Atmospheric Administration (NOAA)

https://doi.org/10.1021/acs.analchem.1c01103
Anal. Chem. 2021, 93, 10141−10151

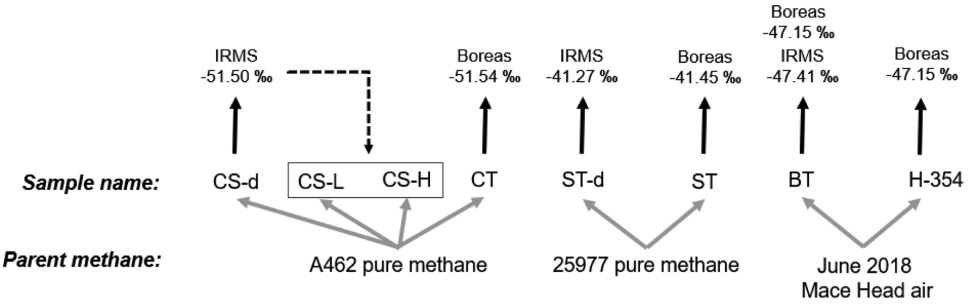

Figure 4. Schematic of the relationship between the parent CH_4, AF PRMs, whole air standards, and measurements made for $\delta^{13}C$. Gray arrows represent physical dilution of the parent CH_4 for preparation of the AF PRMs. All Boreas measurements shown here are made using calibration of the spectrometer via the two synthetic mixtures CS-L and CS-H with 500 μmol mol^{-1} and 626 μmol mol^{-1} amount fractions in N_2, respectively.

procedures for certified reference materials involving processes of cylinder conditioning and venting before a final fill to ~200 bar.[19] The cylinders were filled under conditions of atmospheric transport from the Atlantic that were representative of the well-mixed high latitudes of the Northern Hemisphere.

A sample of each pure CH_4 parent, diluted to near-ambient amount fraction in N_2 (CS-d and ST-d), and the whole air standard BT were analyzed at the Royal Holloway University of London (RHUL) for $\delta^{13}C$, as described in Supporting Information S4. $\delta^{13}C$ has been assigned for the calibration standards by IRMS measurement; however, δ^2H has not been directly measured. We estimate an assignment for δ^2H by reference of the whole air standard to the Northern Hemisphere background value, as described in Supporting Information S4.

2.3.5. Isotope Ratio Definition and Notation. The isotope ratio applied to molecular species quantifies the proportion of molecules containing the rare isotope relative to the most abundant, and this is expressed relative to the same ratio for a reference material

$$\delta^{13}C = \frac{Y_{311}/Y_{211}}{R_{VPDB}} - 1 \quad (1)$$

$$\delta^{13}H = \frac{Y_{212}/Y_{211}}{R_{VSMOW}} - 1 \quad (2)$$

where $Y_{211} \equiv Y(^{12}CH_4)$, $Y_{311} \equiv Y(^{13}CH_4)$, and $Y_{212} \equiv Y(^{12}CH_4D)$ are the calibrated amount fractions of $^{13}CH_4$, $^{12}CH_4$, and $^{12}CH_3D$, respectively (following the notation in Griffith[17] and IUPAC where the symbol X_i is used for the mole fraction of isotopologue i—the proportion relative to all isotopologues—and Y_i for the amount fraction of the isotopologue—the proportion relative to the gas mixture composition; and the Air Force Geophysics Laboratory, AFGL, shorthand notation for isotopologues). Isotope ratios assigned by IRMS are the bulk values, that is, the ratio for all carbon or hydrogen in the sample. The spectrometer measures isotopologues separately, the ratios are referenced to these specific molecules and neglect non-stochastic partitioning of isotopes among the 10 stable isotopologues of CH_4. Recently, there have been significant developments in "clumped" isotopic CH_4 geochemistry, and it is likely that any difference between bulk isotope ratios and isotopologue ratios is below the experimental uncertainty of our measurements.[20] For conciseness, we keep the notation $\delta^{13}C$ to refer to $\delta^{13}C$ (CH_4) and δ^2H to refer to $\delta^2H(CH_4)$, when discussing results.

2.3.6. Calibration Method. There are two approaches to calibrate an instrument response to produce a calibrated isotope ratio, for example, $\delta^{13}C$ relative to the VPDB scale, that relates to the order of operations. The first method is to calibrate the measured isotopologue amount fraction of $^{13}CH_4$ and $^{12}CH_4$ using amount fraction standards and then calculate the ratio of these quantities by eq 1; this is termed as the isotopologue method here. The second method, analogous to that used in IRMS, is to calculate the ratio of instrument responses, $^{13}CH_4$ to $^{12}CH_4$ (i.e., $r = I_{311}/I_{211}$) and then calibrate this ratio using an isotopic standard (here termed as the ratio method).

In IRMS, first calculating the ratio of instrument responses to $^{13}CH_4$ and $^{12}CH_4$ reduces common-mode noise in the measurement, most notably the mass-dependent isotopic fractionation effects due to incomplete transmission of ions through the mass spectrometer. Laser spectrometers, however, make independent absolute measurements of the amount fraction of each isotopologue, and calibration of this quantity and calculation of the isotope ratio have been thoroughly examined for CO_2 isotopologue spectrometers.[18,21] Here, we apply the same principles to calibrate our CH_4 isotopologue spectrometer. The uncalibrated instrument response varies linearly with the amount fraction for each isotopologue independently

$$I_{211} = a_{211}Y_{211} + b_{211} \quad (3)$$

$$I_{311} = a_{311}Y_{311} + b_{311} \quad (4)$$

$$I_{212} = a_{212}Y_{212} + b_{212} \quad (5)$$

The calibration values, gradient (a_i) and intercept (b_i), are determined for each isotopologue using the pair of AF PRMs, CS-L and CS-H (listed in Table 1) and are recalculated for each cycle of the instrument. The isotopologue amount fractions Y_{211}, Y_{311}, and Y_{212} for the calibration standards are determined from the gravimetric amount fraction and the assigned $\delta^{13}C$ and δ^2H, using the method described in Supporting Information S3. Each AF PRM is analyzed within an instrument cycle (Figure 2). The calibration parameters show a drift between runs, which we account for by linearly interpolating values for a_i and b_i over time. The calibration standards, CS-L and CS-H, bracket the samples (after preconcentration) in the total CH_4 amount fraction and are produced from the same pure CH_4 source (Figure 4). The assignment of $\delta^{13}C$ and δ^2H to these calibration gases is described in Supporting Information S4.

We also calibrate the spectrometer using the ratio method, which is sometimes applied to optical measurements, to

https://doi.org/10.1021/acs.analchem.1c01103
Anal. Chem. 2021, 93, 10141−10151

Table 2. Isotopic Ratio and Associated Repeatabilities of the Target Sample Measurements

		δ^{13}C (‰)			δ^{2}H (‰)		
target tank	calibration method	mean	repeatability (1SD)[a]	average rolling repeatability (1SD)[b]	mean	repeatability (1SD)[a]	average rolling repeatability (1SD)[b]
calibration target	*ratio*	−51.54	0.055	0.033	−192.79	0.22	0.17
	isotopologue	−51.54	0.055	0.033	−192.66	0.29	0.27
spectrometer target	*ratio*	−41.47	0.057	0.038	−191.05	0.28	0.20
	isotopologue	−41.45	0.057	0.038	−190.46	0.29	0.27
Boreas target	*ratio*	−47.15	0.079	0.055	−90.48	1.18	0.61
	isotopologue	−47.14	0.083	0.048	−92.63	1.32	0.74

[a]Repeatability of measurements over seven days from 17th to 23rd December 2020. The number of measurements was 116, 116, and 58 for the calibration target, spectrometer target, and Boreas target, respectively. [b]A repeatability of four sequential measurements was calculated, and these were averaged across the same six days.

highlight any resulting differences in these two calibration approaches (Supporting Information S3).

3. RESULTS AND DISCUSSION

3.1. Calibration and Target Sample Analysis. We have characterized the performance of Boreas for measurements of each isotope ratio using the high AF PRMs (CT and ST) in N_2 to verify the calibration accuracy and measurement repeatability of the Aerodyne spectrometer directly and the whole air standards (BT and H-354) to characterize the combined preconcentrator and spectrometer. δ^{13}C has been measured for the AF PRM parent CH_4 and whole air standard, so a direct comparison is made. δ^{2}H has not been measured by IRMS for any of the gases here, so only stability with respect to drift has been characterized.

3.1.1. δ^{13}C Analysis. 3.1.1.1. Spectrometer Characterization. The ratio and isotopologue calibration methods for Boreas show negligible differences in the calibrated values and precision for measurements of δ^{13}C (Table 2). The assumption of linearity in the calibration approach was tested using the CT tank at 550 μmol mol^{-1} CH_4 amount fraction, within the range of the two calibration AF PRMs, CS-L and CS-H (500 and 626 μmol mol^{-1}), all prepared from the same parent CH_4 A462. Multiple analyses (n = 116) over the period of 1 week measured a difference of 0.04 ± 0.05‰ (1SD) from the expected value.

We apply the same calibration procedure for analysis of the spectrometer target AF PRM (ST), made from parent CH_4 25977. Measurements made by IRMS show a difference of 10.23 ± 0.07‰ (1SD) between ST-d and CS-d (see Figure 4 for relationship between parent CH_4, high AF PRMs, and near-ambient amount fraction samples). Our measurements using the spectrometer found a difference of 10.07 ± 0.08‰ for the ratio calibration method and 10.09 ± 0.08‰ for the isotopologue calibration method. The magnitude of difference between IRMS and the spectrometer is very small given the repeatability, shown as one standard deviation of many measurements. There are numerous other factors that could introduce a systematic difference between the measurements made by IRMS and Boreas's spectrometer, which are not accounted for when using repeatability as a simple measure of standard uncertainty. The assumed linearity over the range of amount fractions is validated by measurement of the CT, and a full uncertainty budget analysis is beyond the scope of this study; however, we explain some of the possible reasons. A major factor is the procedure for calibration; Boreas's spectrometer is directly measuring the difference between the ST and CT; however, the IRMS measurements are made relative to a working standard that is changed on a near-annual basis after around 2500 analyses. Small errors in any steps could propagate into a difference of this magnitude. Other contributing factors to the difference could include fractionation or contamination during preparations of the dilutions from both A462 and 25977 (Figure 4). Also, differences due to the measurement of bulk isotope ratios (IRMS) versus a specific isotopologue ratio (laser spectroscopy) due to non-stochastic polyisotopic distributions could be a contributing factor. In this analysis of the ST, we show that Boreas' laser spectrometer makes a robust measurement of isotopically distinct CH_4 using AF PRMs of CH_4 of only a single isotopic composition for calibration. The difference we observe between samples with such a distinct isotopic composition (relative to our IRMS analysis) agrees favorably with the magnitude of differences seen across IRMS laboratories that employ more comparable and mature practices in measurement.[7]

3.1.1.2. Preconcentrator Characterization. To make a similar performance characterization for ambient air samples (processed through the Boreas sampling and preconcentration system), we used analysis of the BT and H-354. Measurement of the BT and H-354 on Boreas showed an identical carbon isotopic composition (difference of 0.00 ± 0.10‰, 1SD). Analysis of H-354 by IRMS measured lighter by 0.26 ± 0.07‰ (1SD) compared to Boreas—a small but significant difference. The reasons for such differences have been studied by the isotopic measurement community, and such variations have often been attributed to the referencing strategy used, with the strategy of "identical treatment" for the sample and reference now being largely employed.[22]

Boreas attempts to process the air sample in a way as to create a pure CH_4 sample in N_2 to matrix match with the spectrometer calibration AF PRMs (CS-L and CS-H). If we assumed that the analysis by IRMS is more accurate than that using Boreas, then it is likely that the Boreas sample is therefore not sufficiently matrix matched. There is evidence for this in our analysis as the repeatability of the BT is not as good as that of the ST (AF PRM with pure CH_4 in N_2), indicating that there is very slight variability in a matrix component that is not being accounted for in calibration. This has also been found to be the case in other studies utilizing preconcentration methods. Eyer et al.[12] found a 2.3‰ offset in their analyses using a similar approach of preconcentration coupled to a laser spectrometer that they attributed to an increase in O_2 in their sample matrix to 40% relative to the standards containing 20%. They also show a decrease in performance between the laser spectrometer (0.1‰ precision estimated from Allan Variance)

https://doi.org/10.1021/acs.analchem.1c01103
Anal. Chem. 2021, 93, 10141−10151

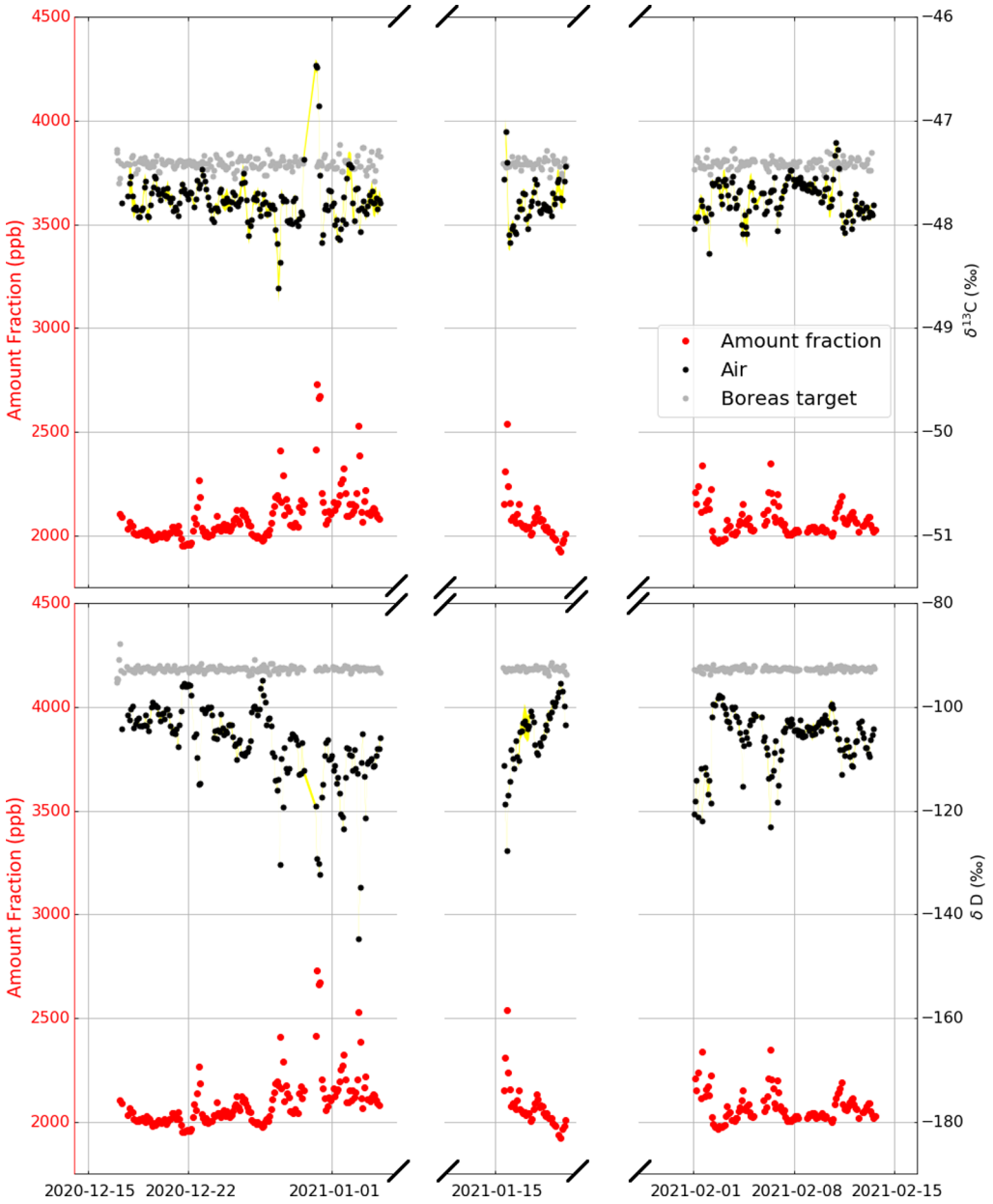

Figure 5. Boreas ambient air time series of $\delta^{13}C$ (top) and $\delta^{2}H$ (bottom) measurements made at NPL from a roof sampling inlet. The same offset is applied to both the BT and air measurements—in this example enabling the $\delta^{13}C$ dataset to be directly comparable to measurements by the RHUL. For $\delta^{2}H$, we have applied an equivalent correction based on an assigned value for the BT of −92.63‰.

and the complete system (0.19‰ repeatability), which they attribute to a variable O_2 content arising from trap temperature control stability. While we have not quantified the matrix effect on Boreas measurements, the 10 mmol mol^{-1} O_2 carryover determined by GC in Section 2.3.2 would produce a 0.12‰ offset relative to our O_2-free standards, assuming the same proportionality.

If and how correction can be made for any offset observed between laboratories is a topic of significant interest in isotope ratio metrology,[7] with much research taking place on how to create both common reference materials and protocols for measurement and analysis. Understanding the origin of remaining inaccuracies in analysis[7,23] is also a topic of interest. To accelerate the combined use of different measurement datasets, a pragmatic approach is often taken. The offset between laboratories is monitored by inter-comparison studies and applied as a correction, which allows the modeling community to utilize the measurements appropriately and without causing biases in the model output. To this end, we measure the BT between every air sample. This allows us to both monitor the stability of the instrument and apply an appropriate, continuously measured offset to the air data to ensure compatibility with at least one IRMS measurement dataset (in our case that of Royal Holloway, University of London; see the Supporting Information). The typical repeatability on the four measurements of the BT spanning a single air measurement is 0.048‰, and thus, applying an offset to each air measurement, we calculate an estimated propagated standard uncertainty on a single air measurement of 0.07‰.

One potential inaccuracy in applying an offset correction is its dependence on the amount fraction in the spectrometer. This would, however, have a negligible influence owing to the

https://doi.org/10.1021/acs.analchem.1c01103
Anal. Chem. 2021, 93, 10141−10151

fact that we only see very small amount fraction dependence in the coefficients of the calibration equations (Supporting Information S3) and that the majority of the calibration is achieved with the synthetic standards.

3.2.1. δ^2H Analysis. There is again evidence of a small, variable matrix effect in the repeatability of the different target samples (CT, ST, and BT). The repeatability of the ST over a week of measurements (0.29‰, 1SD, n = 116) was similar to the average of the 4-point repeatability over the same time period (0.27‰). For the BT, however, long-term repeatability was almost double the average 4-point repeatability at 1.32 and 0.74‰, respectively.

We also found a small but significant difference in the calibrated δ^2H using the ratio or isotopologue methods. We attribute this to the greater amount fraction dependency for the measurement of δ^2H compared with $\delta^{13}C$. $^{12}CH_3D$ is measured using the second laser in the spectrometer, as the absorption signal from this isotopologue is much smaller than that of the more dominant molecules and so is measured in a different region of the spectrum. Also, the strong $^{12}CH_4$ absorption recorded with laser 1 is still used to calculate the ratio r. Consequently, this ratio has a different response in proportion to the amount fraction. The intercept term in the spectrometer calibration (3) for $^{12}CH_4$ (b_{211}) is about 5 μmol mol^{-1}, which is ∼1% of the magnitude under the nominal composition used here; for $^{12}CH_3D$, this is b_{212} = 15 μmol mol^{-1} or ∼4%. This has the effect of increasing the apparent amount fraction dependence of the instrument response ratio I_{212}/I_{211} and limits the accuracy of the phenomenological correction. This correction factor for the deuterated isotopologue is $m(\delta\ D) = 0.0376‰/\mu$mol mol^{-1} compared with $m(\delta\ C\ 13) = -0.00161‰/\mu$mol mol^{-1}. As shown by Griffith,[17] calibration of the δ value obtained directly from the spectrometer response requires a correction term inversely proportional to the amount fraction, so the scaling factor used here is an approximation that is sufficient for only small corrections. The comparison for the calibration target given in Table 2 indicates that this is the case for $\delta^{13}C$ but not for δ^2H in this instrument, where the isotopologue method produces more accurate results with a smaller difference from the expected values of $\delta^{13}C = -51.50‰$ and $\delta D = -192.70‰$. Note that the overall precision expressed as the repeatability is similar for both, showing that both the isotopologue and ratio calibration methods perform equally with instrumental noise and drift in this laser spectrometer.

3.2. Ambient Air Measurement Time Series. Air is continuously drawn into a laboratory at NPL from a sampling inlet on the roof (17 m above ground level, 51.424149° N, 0.343872° W). Boreas samples from this continuous flow, which minimizes dead volume in the sampling lines and reduces the amount of flushing time needed before Boreas begins sampling. Our analysis period spans from mid-December 2020 to mid-February 2021. During this time, there are two breaks in the measurements. On 24th December, the repeatability began to deteriorate as was seen in both the ST measurements (sample loaded straight into the spectrometer) and the BT measurements, indicating an issue with the spectrometer rather than the sampling and preconcentration. The spectrometer laser path was readjusted, and characteristic performance of the instrument resumed. This is a highly unusual intervention that should only be required very rarely. Shortly after this, however, a hardware fault in the sampling system took the instrument offline until mid-January. Once characteristic performance resumed, the instrument was taken offline for two weeks for further tests of the system and analyses (e.g., measurement of H-354 for inter-comparison with IRMS). Following this, the instrument began continuous measurements from 1st February. During this period, there have been no necessary changes of carrier gas, calibration, or target gases. A 40 L (water volume), 200 bar cylinder of N_2 lasts over three months, a 50 L volume 200 bar BT cylinder lasts >6 months (assuming 10 measurements a day), and the 10 L volume 100 bar synthetic AF PRMs last >12 months. Assuming normal operation without faults, Boreas could therefore operate continuously with an optimum calibration strategy for >6 months (assuming automated changeover exists for the N_2 carrier gas or if a N_2 generator was employed). Figure 5 shows the results for $\delta^{13}C$ and δ^2H measurements from this recent period of ambient air analysis. Accurate ambient air amount fraction measurements are critical for quantitative interpretation of the isotope ratios, and our approach with Boreas is explained in Supporting Information S5. The measurements of the BT are also shown to illustrate the repeatability of Boreas relative to the magnitude of changes in ambient air. The standard uncertainty of δ^2H, estimated from the rolling standard deviation of four measurements, relative to the magnitude of changes seen in the atmospheric samples is particularly small as compared with the same dataset for $\delta^{13}C$. Simultaneous analysis of both isotope systems using a single instrument will prove highly valuable for interpretation of atmospheric CH_4 (e.g., as illustrated by Menoud et al.[11] for identifying fossil source CH_4 in Krakow, Poland). The most significant pollution event (occurring at the end of 2020) shows a particularly heavy $\delta^{13}C$ signature, yet a light δ^2H signature is maintained, indicating the significant potential for these measurements for emission source apportionment.

4. CONCLUSIONS

We have developed an instrument that is able to monitor both $\delta^{13}C$ and δ^2H simultaneously in ambient air. We have devised a continuous instrument calibration procedure that is able to estimate the standard uncertainty of each ambient air measurement, based on the measurements of a suite of synthetic AF PRMs and compressed whole air working standards. The system is fully automated, able to make a single air measurement at least every 150 min (based on every sample bracketed by a compressed whole air standard), which is of a frequency that allows for coupling to high- temporal and spatial resolution atmospheric transport models. The additional information provided through isotopic analyses could help quantitatively estimate sectoral emissions of CH_4 from country to regional scales, providing a tool for policy makers looking to make the most efficient gains in emission reductions over the coming years. Analytically, there is potential for the instrument to improve further in precision and accuracy of measurement and to rival IRMS measurement as a high-specification instrument able to continuously measure more than one isotope system simultaneously with low maintenance cost. The performance for δ^2H is particularly favorable relative to that of IRMS analysis and opens up the possibility for in situ high-precision global measurements of δ^2H at remote monitoring observatories.

https://doi.org/10.1021/acs.analchem.1c01103
Anal. Chem. 2021, 93, 10141−10151

■ ASSOCIATED CONTENT

Supporting Information

The Supporting Information is available free of charge at https://pubs.acs.org/doi/10.1021/acs.analchem.1c01103.

CH_4 absorption spectrum recorded in this work and details of the fitting procedure; stability of the spectrometer measurement, used to determine the optimum averaging duration; mathematical description of the isotopologue and isotope ratio calibration methods; mass spectrometry measurements and international scale linkage; and calculation of CH_4 amount fractions in ambient air (PDF)

■ AUTHOR INFORMATION

Corresponding Author

Tim Arnold − *National Physical Laboratory, Teddington TW11 0LW Middlesex, U.K.; School of GeoSciences, University of Edinburgh, Edinburgh EH8 9XP, U.K.;* orcid.org/0000-0001-9097-8907; Email: tim.arnold@npl.co.uk

Authors

Chris Rennick − *National Physical Laboratory, Teddington TW11 0LW Middlesex, U.K.*

Emmal Safi − *National Physical Laboratory, Teddington TW11 0LW Middlesex, U.K.; School of GeoSciences, University of Edinburgh, Edinburgh EH8 9XP, U.K.*

Alice Drinkwater − *National Physical Laboratory, Teddington TW11 0LW Middlesex, U.K.; School of GeoSciences, University of Edinburgh, Edinburgh EH8 9XP, U.K.*

Caroline Dylag − *National Physical Laboratory, Teddington TW11 0LW Middlesex, U.K.*

Eric Mussell Webber − *National Physical Laboratory, Teddington TW11 0LW Middlesex, U.K.*

Ruth Hill-Pearce − *National Physical Laboratory, Teddington TW11 0LW Middlesex, U.K.;* orcid.org/0000-0002-5515-0909

David R. Worton − *National Physical Laboratory, Teddington TW11 0LW Middlesex, U.K.;* orcid.org/0000-0002-6558-5586

Francesco Bausi − *National Physical Laboratory, Teddington TW11 0LW Middlesex, U.K.*

Dave Lowry − *Department of Earth Sciences, Royal Holloway, University of London, Egham TW20 0EY Surrey, U.K.*

Complete contact information is available at: https://pubs.acs.org/10.1021/acs.analchem.1c01103

Notes

The authors declare no competing financial interest.

■ ACKNOWLEDGMENTS

Gerry Spain is gratefully acknowledged for his help filling compressed whole air standards at Mace Head in 2018. Jon Helmore kindly donated a sample of CH_4 from his own experiments, which proved highly valuable. Aerodyne Research Inc has been very generous in helping us resolve any software issues when they arose. We thank Peter Salameh of GCSoft for his support. Funding for this work is primarily through the NPL Directors' Fund, National Measurement System Funding, NERC's DARE-UK project (NE/S003819/1), NERC's POLYGRAM project (NE/V007149/1), the EMPIR STELLAR project, and the University of Edinburgh's NERC E3 Doctoral Training Partnership. The 19ENV05 STELLAR project has received funding from the EMPIR programme co-financed by the participating states and from the European Union's Horizon 2020 research and innovation programme.

■ REFERENCES

(1) IPCC. *Climate Change 2013: The Physical Science Basis. Contribution of Working Group I to the Fifth Assessment Report of the Intergovernmental Panel on Climate Change*; Cambridge University Press: Cambridge, United Kingdom and New York, NY, USA, 2013; p 1535.

(2) Turner, A. J.; Frankenberg, C.; Kort, E. A. *Proc. Natl. Acad. Sci.* **2019**, *116*, 2805−2813.

(3) Ganesan, A. L.; Schwietzke, S.; Poulter, B.; Arnold, T.; Lan, X.; Rigby, M.; Vogel, F. R.; Werf, G. R.; Janssens-Maenhout, G.; Boesch, H.; Pandey, S.; Manning, A. J.; Jackson, R. B.; Nisbet, E. G.; Manning, M. R. *Global Biogeochem. Cycles* **2019**, *33*, 1475−1512.

(4) Brenninkmeijer, C. A. M.; Janssen, C.; Kaiser, J.; Röckmann, T.; Rhee, T. S.; Assonov, S. S. *Chem. Rev.* **2003**, *103*, 5125−5162.

(5) Nisbet, E. G.; Manning, M. R.; Dlugokencky, E. J.; Fisher, R. E.; Lowry, D.; Michel, S. E.; Myhre, C. L.; Platt, S. M.; Allen, G.; Bousquet, P.; Brownlow, R.; Cain, M.; France, J. L.; Hermansen, O.; Hossaini, R.; Jones, A. E.; Levin, I.; Manning, A. C.; Myhre, G.; Pyle, J. A.; Vaughn, B. H.; Warwick, N. J.; White, J. W. C. *Global Biogeochem. Cycles* **2019**, *33*, 318−342.

(6) Fisher, R. E.; Sriskantharajah, S.; Lowry, D.; Lanoiselle, M.; Fowler, C. M. R.; James, R. H.; Hermansen, O.; Myhre, C. L.; Stohl, A.; Greinert, J.; Nisbet-Jones, P. B. R.; Mienert, J.; Nisbet, E. G. *Geophys. Res. Lett.* **2011**, *38*, L21803.

(7) Umezawa, T.; Brenninkmeijer, C. A. M.; Röckmann, T.; van der Veen, C.; Tyler, S. C.; Fujita, R.; Morimoto, S.; Aoki, S.; Sowers, T.; Schmitt, J.; Bock, M.; Beck, J.; Fischer, H.; Michel, S. E.; Vaughn, B. H.; Miller, J. B.; White, J. W. C.; Brailsford, G.; Schaefer, H.; Sperlich, P.; Brand, W. A.; Rothe, M.; Blunier, T.; Lowry, D.; Fisher, R. E.; Nisbet, E. G.; Rice, A. L.; Bergamaschi, P.; Veidt, C.; Levin, I. *Atmos. Meas. Tech.* **2018**, *11*, 1207−1231.

(8) Rigby, M.; Manning, A. J.; Prinn, R. G. *J. Geophys. Res.: Atmos.* **2012**, *117*, D12312.

(9) Röckmann, T.; Eyer, S.; van der Veen, C.; Popa, M. E.; Tuzson, B.; Monteil, G.; Houweling, S.; Harris, E.; Brunner, D.; Fischer, H.; Zazzeri, G.; Lowry, D.; Nisbet, E. G.; Brand, W. A.; Necki, J. M.; Emmenegger, L.; Mohn, J. *Atmos. Chem. Phys.* **2016**, *16*, 10469−10487.

(10) Menoud, M.; van der Veen, C.; Scheeren, B.; Chen, H.; Szénási, B.; Morales, R. P.; Pison, I.; Bousquet, P.; Brunner, D.; Röckmann, T. *Tellus B* **2020**, *72*, 1−20.

(11) Menoud, M.; van der Veen, C.; Necki, J.; Bartyzel, J.; Szénási, B.; Stanisavljević, M.; Pison, I.; Bousquet, P.; Röckmann, T. *Atmos. Chem. Phys. Discuss.* **2021**, *2021*, 1−31.

(12) Eyer, S.; Tuzson, B.; Popa, M. E.; van der Veen, C.; Röckmann, T.; Rothe, M.; Brand, W. A.; Fisher, R.; Lowry, D.; Nisbet, E. G.; Brennwald, M. S.; Harris, E.; Zellweger, C.; Emmenegger, L.; Fischer, H.; Mohn, J. *Atmos. Meas. Tech.* **2016**, *9*, 263−280.

(13) Gordon, I. E.; Rothman, L. S.; Hill, C.; Kochanov, R. V.; Tan, Y.; Bernath, P. F.; Birk, M.; Boudon, V.; Campargue, A.; Chance, K. V.; Drouin, B. J.; Flaud, J.-M.; Gamache, R. R.; Hodges, J. T.; Jacquemart, D.; Perevalov, V. I.; Perrin, A.; Shine, K. P.; Smith, M.-A. H.; Tennyson, J.; Toon, G. C.; Tran, H.; Tyuterev, V. G.; Barbe, A.; Császár, A. G.; Devi, V. M.; Furtenbacher, T.; Harrison, J. J.; Hartmann, J.-M.; Jolly, A.; Johnson, T. J.; Karman, T.; Kleiner, I.; Kyuberis, A. A.; Loos, J.; Lyulin, O. M.; Massie, S. T.; Mikhailenko, S. N.; Moazzen-Ahmadi, N.; Müller, H. S. P.; Naumenko, O. V.; Nikitin, A. V.; Polyansky, O. L.; Rey, M.; Rotger, M.; Sharpe, S. W.; Sung, K.; Starikova, E.; Tashkun, S. A.; Auwera, J. V.; Wagner, G.; Wilzewski, J.; Wcisło, P.; Yu, S.; Zak, E. J. *J. Quant. Spectrosc. Radiat. Transf.* **2017**, *203*, 3−69.

(14) Miller, B. R.; Weiss, R. F.; Salameh, P. K.; Tanhua, T.; Greally, B. R.; Mühle, J.; Simmonds, P. G. *Anal. Chem.* **2008**, *80*, 1536−1545.

(15) Arnold, T.; Mühle, J.; Salameh, P. K.; Harth, C. M.; Ivy, D. J.; Weiss, R. F. *Anal. Chem.* **2012**, *84*, 4798−4804.
(16) Mohn, J.; Guggenheim, C.; Tuzson, B.; Vollmer, M. K.; Toyoda, S.; Yoshida, N.; Emmenegger, L. *Atmos. Meas. Tech.* **2010**, *3*, 609−618.
(17) Griffith, D. W. T. *Atmos. Meas. Tech.* **2018**, *11*, 6189−6201.
(18) Flores, E.; Viallon, J.; Moussay, P.; Griffith, D. W. T.; Wielgosz, R. I. *Anal. Chem.* **2017**, *89*, 3648−3655.
(19) Kitzis, D. *Preparation and Stability of Standard Reference Air Mixtures*; Central Calibration Laboratory. 2017(accessed 16th February 2021).
(20) Douglas, P. M. J.; Stolper, D. A.; Eiler, J. M.; Sessions, A. L.; Lawson, M.; Shuai, Y.; Bishop, A.; Podlaha, O. G.; Ferreira, A. A.; Santos Neto, E. V.; Niemann, M.; Steen, A. S.; Huang, L.; Chimiak, L.; Valentine, D. L.; Fiebig, J.; Luhmann, A. J.; Seyfried, W. E.; Etiope, G.; Schoell, M.; Inskeep, W. P.; Moran, J. J.; Kitchen, N. *Org. Geochem.* **2017**, *113*, 262−282.
(21) Wen, X.-F.; Meng, Y.; Zhang, X.-Y.; Sun, X.-M.; Lee, X. *Atmos. Meas. Tech.* **2013**, *6*, 1491−1501.
(22) Werner, R. A.; Brand, W. A. *Rapid Commun. Mass Spectrom.* **2001**, *15*, 501−519.
(23) Sperlich, P.; Uitslag, N. A. M.; Richter, J. M.; Rothe, M.; Geilmann, H.; van der Veen, C.; Röckmann, T.; Blunier, T.; Brand, W. A. *Atmos. Meas. Tech.* **2016**, *9*, 3717−3737.

https://doi.org/10.1021/acs.analchem.1c01103
Anal. Chem. 2021, 93, 10141−10151